JMES The International Journal of
Mechanical Engineering and Sciences
https://iptek.its.ac.id/index.php/jmes
e-ISSN 2580-7471

Numerical Study of Damper Plate and Nozzle Effect on Vortex Turbine Basin for Increasing Flow Kinetic Energy Entering Turbine Rotor

Herman Sasongko, Wildan Alfa Rahman*

Department of Mechanical Engineering, Institut Teknologi Sepuluh Nopember, Sukolilo Surabaya 60111, Indonesia

Received: 22 February 2023, Revised: 20 March 2023, Accepted: 23 March 2023

Abstract

The Gravitational Water Vortex Power Plant (GWVPP) is a small-scale hydroelectric power generator that uses the energy generated from a vortex flow to turn turbine blades and generate electricity. In this research study, the focus was on the numerical analysis of the basin design of the GWVPP, which was divided into three sections: vortex generator, transformer, and turbine. To support the transformation process from tangential vortex speed to axial vortex speed in the transformer section, a damper plate was installed to direct the rotating flow. The effect of the nozzle in accelerating the flow for optimizing the basin design was also studied to reduce blockage caused by the transformation process. The numerical results indicate that the basin design with a nozzle had lower velocity output due to blockage from the rotating flow. At a flow rate of 0.1 m^3/s, the damper plate reduced the maximum flow rotation, but at a flow rate of 0.2 m^3/s, it prevented flow leakage on the surface. The basin design without a damper plate and a nozzle was the optimal variation for flow rates of 0.1 m^3/s, while the design with a damper plate without a nozzle was optimal for flow rates of 0.2 m^3/s.

Keywords: Gravitational Water Vortex Power Plant (GWVPP), transformer section, damper plate, nozzle

1. Introduction

When examining irrigation rivers with a low head but a sufficient flow rate to be considered viable, a hydropower potential exists. The Central Statistics Agency (BPS) [1] data shows that 108 rivers with a catchment area of 100 km^2 are spread throughout Indonesia, possessing high flow rates but lacking a sufficient head. This abundance of flow rate in such rivers indicates potential for hydropower which can be harvested by mini/micro-hydropower technologies such as Gravitational Water Vortex Power Plant (GWVPP). This plant rotates straight water flow to generate tangential kinetic energy, which rotates the turbine, allowing for a very low head operation.

The Gravitational Water Vortex Power Plant (GWVPP) was first introduced by Brown [2], who demonstrated that "vortical forces" generated by fluid flow could create power. Brown's example employed a square water path with a sloping baffle on its wall and small holes at the bottom as the water outlet. The sloping baffle defined the direction of the whirlpool created by the tangential flow of the outlet. An impeller with a pedal shape was then attached to the hole, and the rotational motion of the whirlpool caused the impeller to rotate.

Brown [2] proved that a water vortex had the potential as an alternative renewable energy source. The process of harnessing the dynamic energy of a water vortex begins with vortex formation in the basin, which is then transformed into axial kinetic energy and used to rotate the axial turbine underneath. This method is suitable for rivers with a low head because the potential static energy of the river water is not immediately used but is rotated first into a dynamic energy vortex before being used to rotate the turbine. Micro-hydropower technology can utilize this concept to support the electrification of areas surrounding the river flow.

Timilsina et al. [3] provided a summary of various research studies on the current trends in hydropower technology development. According to their research, hydropower technology development in recent years has focused on low-head hydropower, particularly on the Gravitational Water Vortex Power Plant (GWVPP). They also noted the need for more detailed numerical modelling of multiphase flow to further understand the flow concept in GWVPP.

Wanchat et al. [4] investigated the essential parameters for optimizing the design process of GWVPP. They found that the critical parameter to consider is the outlet diameter, and for a cylindrical basin with a 1-meter height, the suitable diameter for the outlet was 0.2-0.3 meters to achieve a vortex surface height of 0.3-0.4 meters.

*Corresponding author. Email: alfawildan@gmail.com

Power et al. [5] presented their findings on the maximum efficiency of a cylindrical GWVPP basin with impulse turbines. Their experiments showed a 15.1% maximum efficiency with a flow rate of 0.65 L/s and an inlet height of 25 cm. They used a bladed turbine with a maximum area and 60% resistance force of the maximum flow force. However, the results require additional validation for optimal blade and basin geometry. Dhakal et al. [6] compared the cylindrical and conical basin designs for the Water Vortex Hydropower system. Using numerical methods and experiments, they evaluated the power output of both basin shapes under the same parameter values. They found that the conical basin shape had superior efficiency under the same inlet and outlet conditions, both numerically and experimentally.

Dhakal et al. [7] studied the geometry conditions for optimal GWVPP installation in a conical basin. They sought to establish clear parameters for the basin geometry, as it could be expensive without specific standards. They used numerical and experimental methods to determine the optimal ratio between basin diameter (D) and outlet diameter (d). Their results showed that the optimal d/D ratio was 20-25%, based on numerical analysis with ANSYS CFX. The experimental results supported this finding, with the highest power output occurring at d/D ratios of 20% and 25%. Therefore, they concluded that the optimal d/D ratio for a conical basin was between 20-25%.

In different research conducted by Wardhana et al. [8], they studied the propeller design for GWVPP and examined the impact of the airfoil turbine's geometry on its output power. They used the Gottingen 428 airfoil, varying the chord length and angle of attack with a twist angle of 40°. A numerical analysis on a cylindrical basin using ANSYS Fluent found that a twisted turbine achieved the highest efficiency at 54.40%. The number of blades and airfoil geometry also affected the output power of the GWVPP.

The study conducted by Powalla et al. [9] aimed to develop a numerical model of a vortex turbine that could be used as a reference for further research on the performance of vortex turbines. The study was conducted numerically with validation in the form of experimental data collected from a full-scale prototype installed at TU Dresden, Germany. The simulation was conducted under an unsteady multiphase volume of fluid conditions with an inlet of 0.7 m^3/s. The results obtained by Powalla showed that the multiphase numerical modelling could well model the on-site installation conditions. The results showed that the maximum velocity in the turbine house was at 2.5 m/s, both in installation and numerical models, with the highest vortex height at 1-1.25 m.

Based on the studies above, further research on the development of GWVPP design is needed. The problem with GWVPP using axial turbines as the energy converter from vortex motion to electrical energy is that the current vortex generators cannot maximize the output power of the flow that the turbine absorbs. This weakness occurs due to the possibility of flow blockage caused by the presence of the turbine.

By dividing the basin into three sections: vortex generator section, transformer section, and turbine section, as shown in Figure 1, it is hoped that the water flow rotated into a vortex can be optimized. In the vortex generator, tangential vortex energy is generated and then transformed into axial energy in the transformer section to be used by an axial turbine in the turbine section.

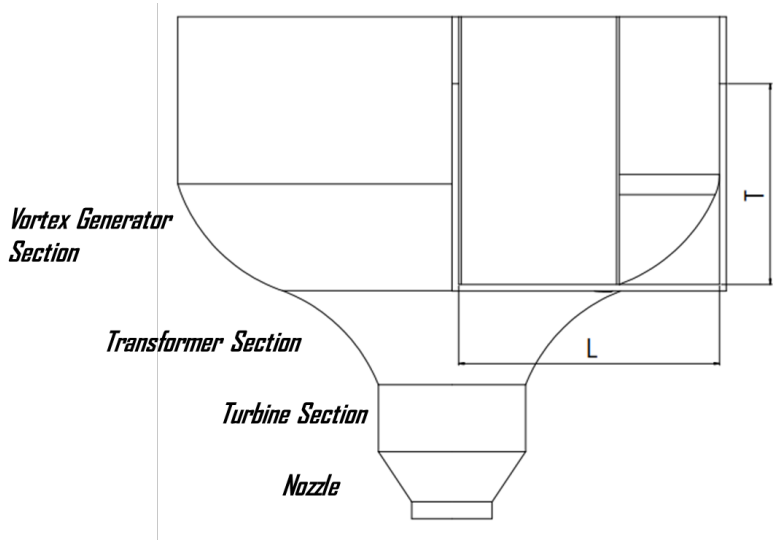

Figure 1. Basin main part.

To improve the transformation process in the transformer section, a damper plate is used to direct the flow and prevent collisions between the rotating and incoming flows. This helps to move the rotating flow quickly towards the transformer section for transformation. Additionally, the impact of the nozzle on flow acceleration needs to be studied to minimize blockage and enhance the basin design.

2. Method

This research on the design of the Gravitational Water Vortex Power Plant (GWVPP) basin was conducted using numerical computation methods. The numerical computation method consisted of three stages: pre-processing, solver/processing, and post-processing. Pre-processing was the stage of preparing the simulation domain. Processing was the core stage of the simulation, where iterations were performed to solve the Navier-Stokes equations in cylindrical coordinates that represented the system equations. The final simulation results were processed in the post-processing stage to extract qualitative and quantitative data to be interpreted later. Software used in this numerical computation method included Solidworks 2016 X64 Edition, ANSYS ICEM 19, and ANSYS FLUENT 19 [10, 11].

In performing the simulation, the domain geometry was the GWVPP basin design geometry, which was created using Solidworks 2016 X64 Edition, and then the flow domain was extracted using ANSYS Design Modeler. The simulation domain was meshed using ANSYS ICEM 19. The simulation domain size used was as shown in shown in Figure 2, with detailed dimensions provided in Table 1. Variations in the simulation is shown in Table 2 where in every geometry will be executed in two different flow capacity of 0.1 m^3/s and 0.2 m^3/s.

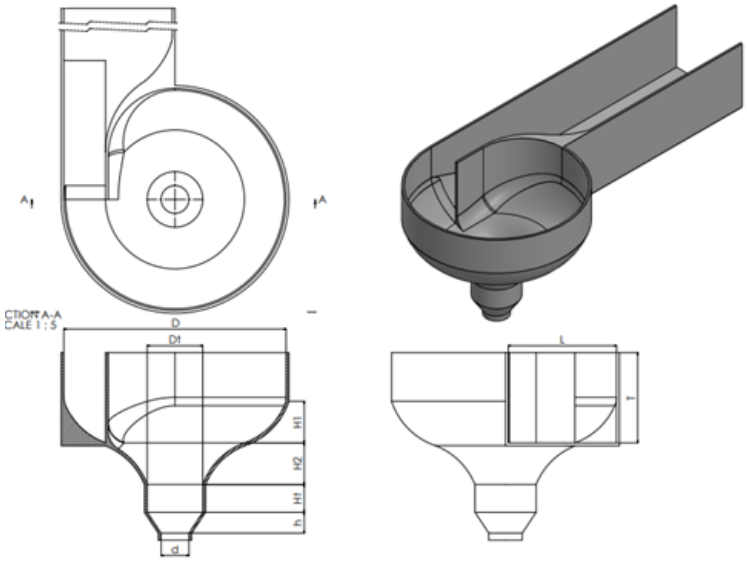

Figure 2. Basin geometry.

Table 1. Geometry data.

Parameter	Symbol	Dimension (mm)
Vortex Generator Diameter	D	1600
Turbine House Diameter	D_t	400
Nozzle Diameter	d	200
Vortex Generator Height	H_1	300
Wall Height	H_w	500
Vortex-Axial Transformer Height	H_2	300
Turbine House Height	H_t	200
Nozzle Height	h	150
Vortex Generator Arc Radius	R_1	500
Vortex-Axial Transformer Arc Radius	R_2	500
Inlet Width	L	780
Inlet Height	T	700

Table 2. Simulation variation.

Variation		Nozzle	
		Present	Not Present
Damper Plate	Present	Basin geometry With Damper Plate and Nozzle	Basin geometry With Damper Plate and Without Nozzle
	Not Present	Basin geometry Without Damper Plate and with Nozzle	Basin geometry Without Damper Plate and Nozzle

The meshing of the simulation was performed using a hexahedron mesh with a total of 561,257 meshes based on the basin design shown in Figure 3. The simulation was carried out in a steady state condition, using a multiphase Volume of Fluid model with RNG k – e turbulent model. The simulation boundary conditions included a free surface modelled with a pressure outlet of 0 Pa at the top, a pressure outlet of 0 Pa at the outlet, and a mass-flow inlet with water flow rates of 0.1 m^3/s and 0.2 m^3/s at the inlet. The model used a no-slip wall condition. The fluid used in the simulation was water, with a density of 998.2 kg/m^3 and air, with a density of 1.225 kg/m^3.

To ensure that the validation of the simulation results did not depend on the mesh density used, a grid independence test was performed to compare the simulation results at each mesh value. Quantitative velocity data was used as a parameter in the grid independence test in this simulation. The grid independence test was conducted on the range number of elements in the mesh from 280,000 to 950,000 elements. As shown in Figure 4, the velocity value no longer showed significant changes when the number of elements was above 544,501. The simulation used the SIMPLE solution method with second-order momentum, turbulent kinetic energy, turbulent dissipation rate, and PRESTO! for pressure. The residual value was targeted to achieve convergence at 10^{-6} in this numerical simulation as a sign of successful simulation or when the average velocity value in the area just before entering the turbine house showed the same value at each iteration.

3. Results and Discussion

In this section, analysis and discussion were conducted to discuss the flow generated in the basin design that utilizes the vortex to axial transformer section. The variations were the presence of a damper plate and nozzle, and each design variation was numerically simulated with inlet flow rates of 0.1 m^3/s and 0.2 m^3/s. The analysis included qualitative data analysis in the form of velocity and pressure contour plots, as well as quantitative data analysis comparing pressure and velocity for each variation. The qualitative data was taken at four sampling points: cross-sectional cuts on the XZ plane at heights of $Y = 0.4$ meters, 0.7 meters, and 1 meter, as well as a vertical cut on the YZ plane at $X = 0$ meters.

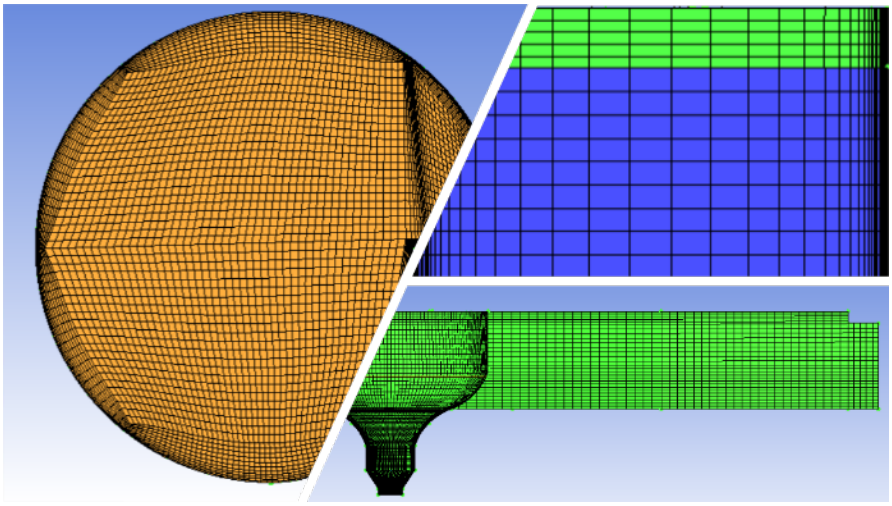

Figure 3. Meshing.

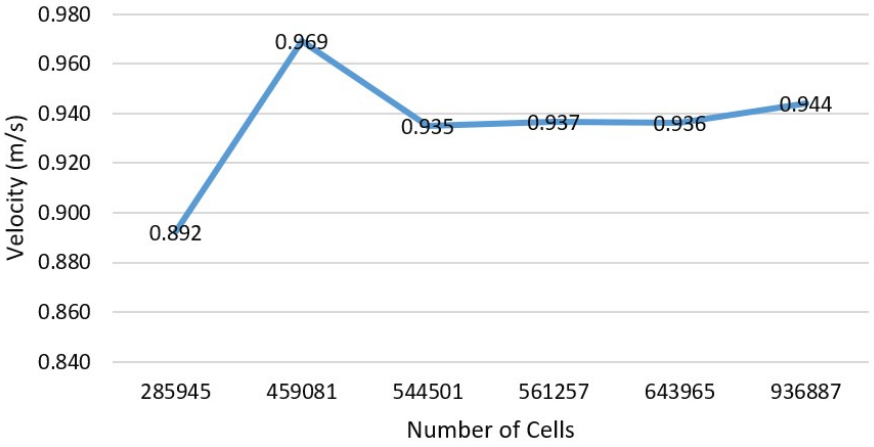

Figure 4. Grid independency test.

As shown in Figure 6, an iso-surface of 0.5 indicated the boundary surface between air and water. The iso-surface was well-formed in the vortex generator section, but in the inlet channel, two images are not perfectly formed shown by Figure 6(a) and Figure 6(b). The first one, Figure 6(a), indicated spillage due to flow obstruction, possibly caused by a collision between the rotating flow in the vortex generator and the incoming flow from the inlet channel.

In Figure 6(b), a phenomenon of "starving debit" is observed, where the water level in the inlet channel and the vortex generator area was lower than the wall, indicating a very smooth flow without any obstruction. This was due to the obstruction of the flow collision at the vortex generator by the damper plate and the outlet condition not experiencing any constriction, suggesting that the design could handle even higher flow debit.

In Figure 6, it was observed that the streamline formed by the inlet flow moved straight and then entered the vortex generator section to be rotated. After rotation, the flow was transformed axially in the transformer section. However, the swirl flow remained, indicating the presence of tangential velocity residual.

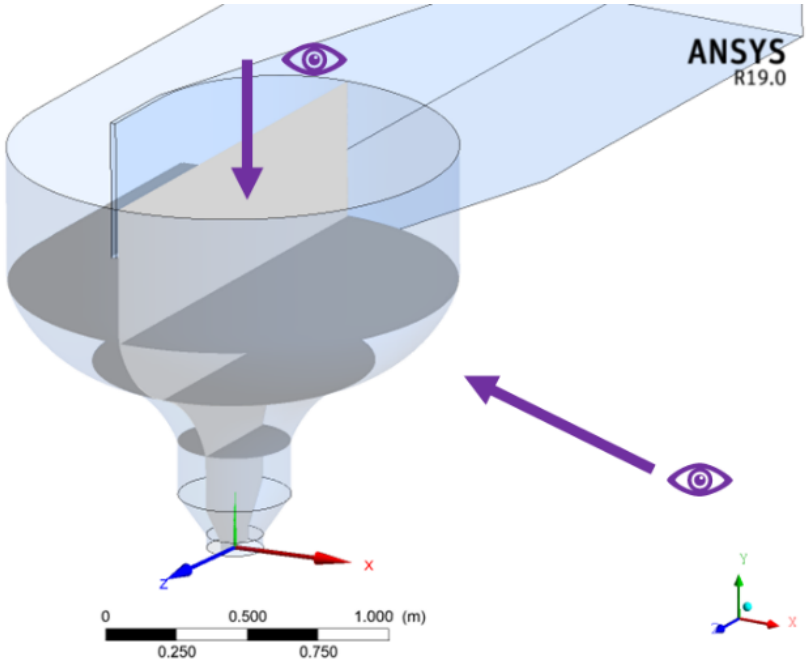

Figure 5. Data sampling location.

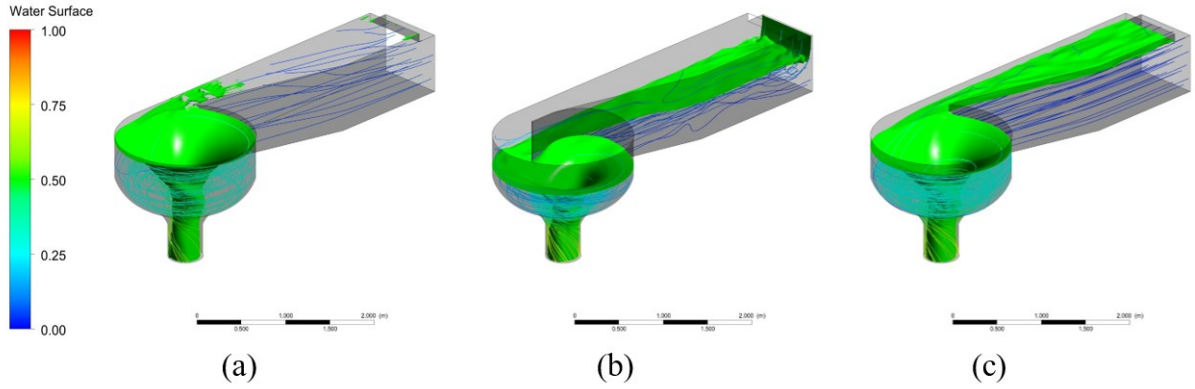

Figure 6. Water surface boundary modelled as iso-surface contours (a) Iso-surface of water spillage condition, (b) Iso-surface of starving debit condition, (c) Iso-surface of perfectly formed flow condition.

In Figure 7, the dominant phase contour colors were red and blue, indicating water and air fractions, respectively. The red contour near the wall was formed due to the centripetal force of the rotating water flow. In the designed basin with a damper plate and a nozzle shown in Figure 7(a), there was a possibility of a shift in the vortex region due to the presence of the nozzle and damper plate, as seen from the formation of a blue contour in the turbine section.

When examining Figure 7(b) of the basin design without a damper plate and with a nozzle, the removal of the damper plate resulted in a neatly formed blue air phase contour in the center area, with no red water phase contour filling it. In the design without a nozzle in Figure 7(c), there was a higher concentration of the air phase in the turbine section compared to when using a nozzle, indicating that the flow became easier to come out without a nozzle, which means that the presence of a nozzle could potentially cause resistance to the flow.

It was more clearly visible that the pressure contour on the basin design with a nozzle showed a high-pressure concentration in the area before the nozzle, as indicated in Figure 8(a) in red and Figure 8(b) in orange. This high pressure indicated a decrease in speed due to the accumulation of water mass caused by the narrowing of the flow cross-section. Figure 8(c) showed a clear difference in the very low pressure formed in the turbine section, as indicated by the dark blue contour. Slightly higher pressure was only formed in the area around the wall, indicating pressure from the flowing water. As shown in Figure 7(c), it was confirmed that the water phase in the turbine house was only around the wall.

Figure 9 showed horizontal XZ slices of velocity contours in the basin at heights of 1 meter, 0.7 meters, and 0.4 meters. The change in contour colors was noticeable as the height decreased. The color change indicated an increase in velocity as the flow height decreased, demonstrating the successful generation of tangential vortex energy in the vortex generator, which was transformed and utilized in the turbine section. The precise observation point was at 0.7 meters, which was located just before entering the transformer section. The middle area of the velocity contours was filled with green color, indicating a free vortex where the smaller the radius of the vortex, the faster the tangential velocity.

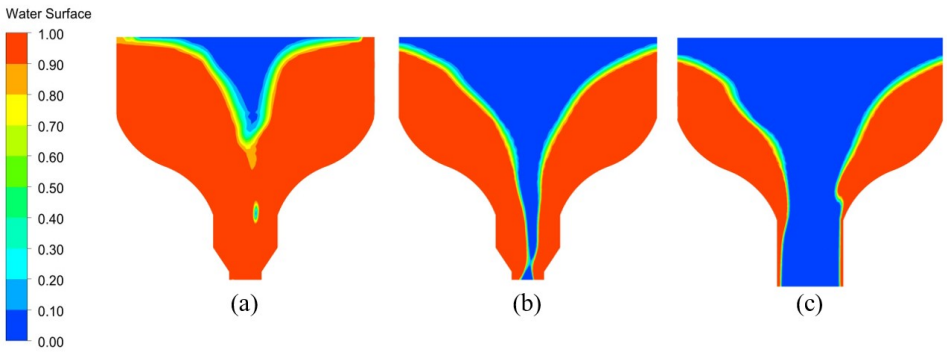

Figure 7. Phase contour of (a) Basin with damper plate and nozzle, (b) Basin without damper plate but with nozzle, (c) Basin without damper plate and nozzle.

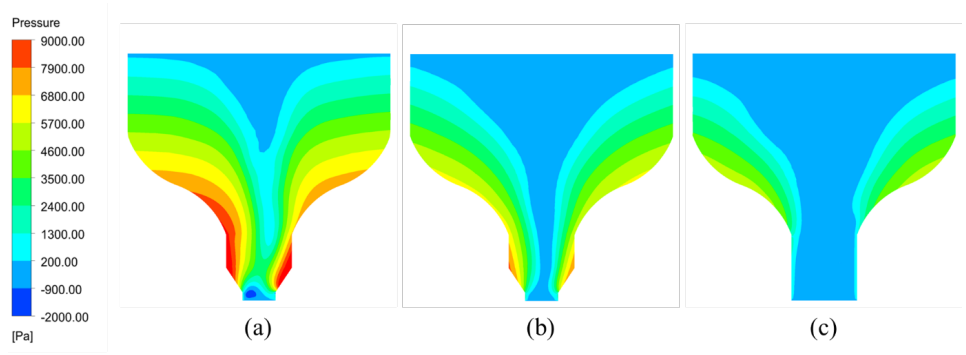

Figure 8. Pressure contour of (a) Basin with damper plate and nozzle, (b) Basin without damper plate but with nozzle, (c) Basin without damper plate and nozzle.

In the absence of damper plates and nozzles Figure 9(b), a brighter blue color was visible in the inlet channel leading to the vortex generator. In contrast with velocity contour when damper plates were added, as shown in Figure 9(a), which resulted in a smaller radius of rotation and immediate transformation. The presence of damper plates was essential for maximizing flow at high capacity, but it should be removed at low capacity to maximize flow.

Figure 10 compared velocity contours for four basin designs and capacity variations at the height of 0.4 meters before entering the axial turbine section. Generally, the velocity contours on the walls had brighter color values than those in the middle.

As illustrated in Figure 10, there was a noticeable difference in the velocity contours between the central area and the walls. This was because the central region was dominated by air, leading to low-velocity contours. Figure 10 displayed the velocity contours for the basin design without nozzles with no "starving debit" condition. The velocity in the basin design with a damper plate at a flow capacity of 0.1 m^3/s was lower than the others due to a starving condition resulting from a lack of flow discharge, as shown in Figure 10(a). Basin design without damper plate and nozzle exhibited similar velocity contours since they shared the same geometry but differed in flow capacity, as shown in Figure 10(b). Similar contours occurred since some of the formed flow with 0.2 m^3/s flow capacity was wasted due to a narrowing inlet channel formed by rotating flow collision that created water spillage, preventing maximum flow rotation. In contrast, the basin design with a damper plate without nozzles at a capacity of 0.2 m^3/s had a brighter velocity contour than other designs due to the damper plate's presence, saving the flow from collision and preventing any flow spillage, as shown in Figure 10(a).

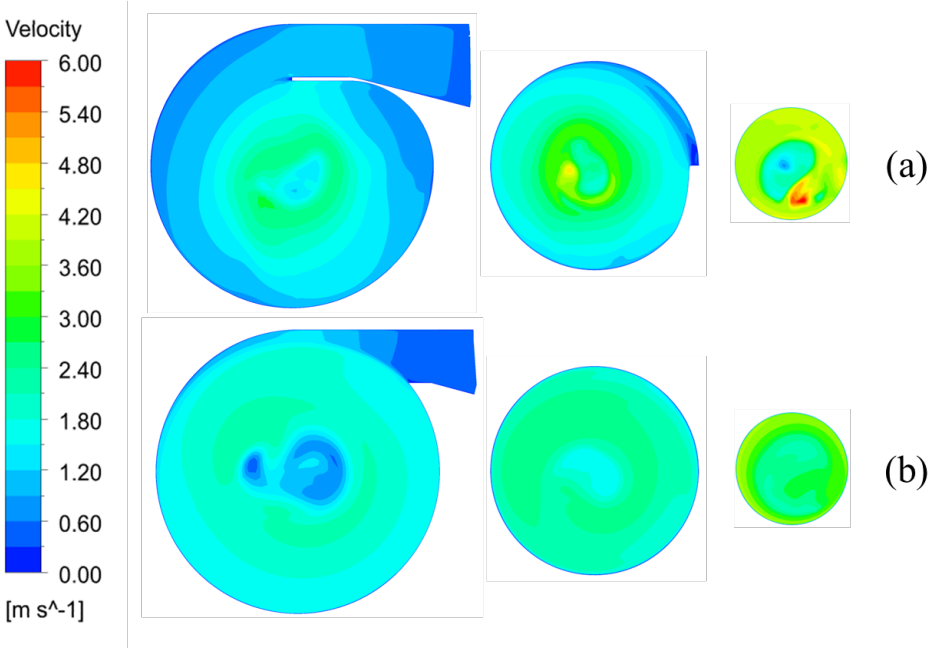

Figure 9. Velocity contour comparison at 1 m, 0.7 m, and 0.4 m (a) Basin with damper plate without nozzle at flow capacity of 0.2 m^3/s, (b) Basin without damper plate and nozzle at flow capacity of 0.1 m^3/s.

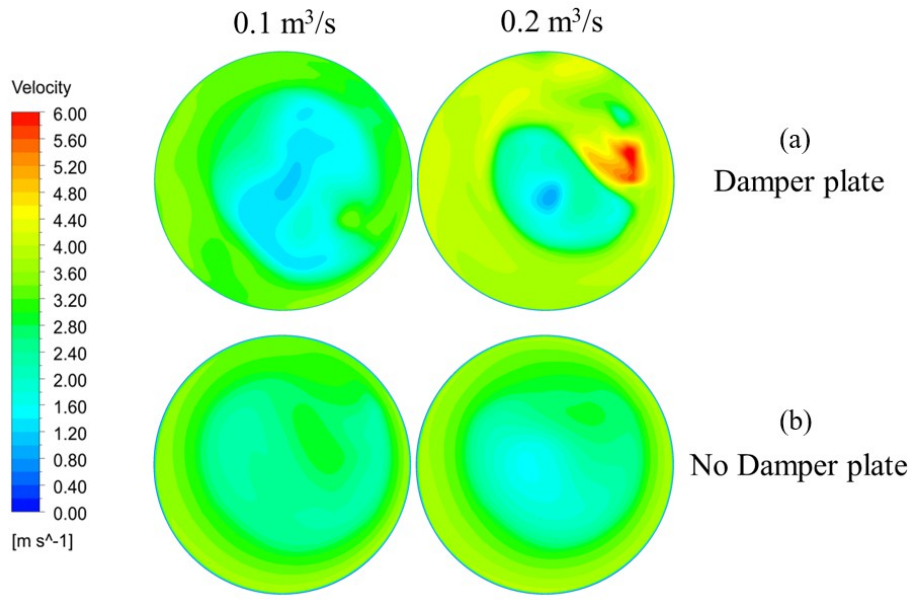

Figure 10. Velocity contour comparison at 0.4 m (a) Basin with damper plate without nozzle, (b) Basin without damper plate and nozzle.

The velocity data in Table 3 displayed variations in the basin designs. Basin designs with nozzles had lower average velocities, namely 2.35 m/s and 2.32 m/s at a capacity of 0.1 m^3/s, and 2.47 m/s and 2.41 m/s at a capacity of 0.2 m^3/s. This was due to the nozzle constricting the flow area, where the rotating flow condition caused blockages in the section.

At a capacity of 0.1 m^3/s, the highest average velocity was found in the basin design without a damper plate and nozzle. This design experienced no flow spillage and had the highest speed increase up to 16.17 times, with a maximum speed of 2.91 m/s. This was consistent with the velocity contour shown in Figure 10, which exhibited the brightest contour at the same capacity. Furthermore, in the basin design with a damper plate but without a nozzle, a "starving debit" condition occurred due to a lack of flow, causing the velocity to decrease to 2.59 m/s.

On the other hand, at a capacity of 0.2 m^3/s, the basin design with a damper plate without a nozzle showed the highest average velocity. This design had no flow spillage and had the highest speed increase up to 9.75 times, with a maximum speed of 3.51 m/s. This was due to the damper plate preventing flow narrowing in the inlet channel, avoiding flow spillage. This was supported by the results of the velocity contour in Figure 10, which exhibited the brightest colour distribution in the velocity contour.

The vertical section of axial (a) and tangential (b) velocity contours in the basin design with a damper plate without a nozzle at a capacity of 0.2 m^3/s is shown in Figure 11. Higher tangential velocity contours dominated the vortex generator and transformer sections. After transformation and entering the turbine house, the velocity contour distribution had the same color value in the basin wall area.

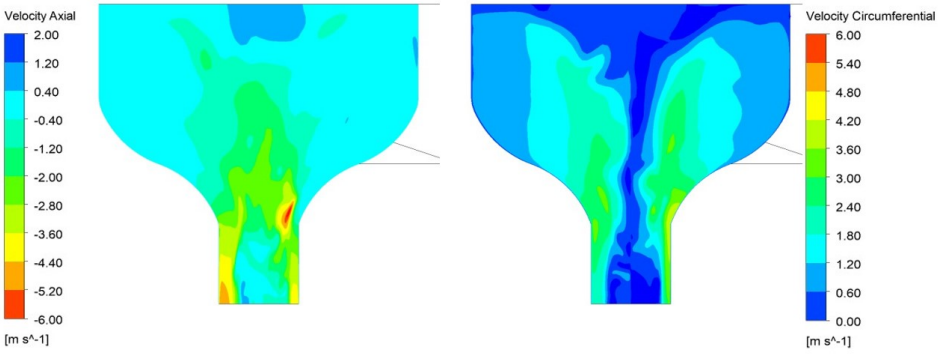

Figure 11. Velocity contour of the basin with damper plate without nozzle at flow capacity of 0.2 m^3/s (a) axial velocity, (b) circumferential velocity.

Table 3. Average velocity at the turbine section entrance.

Flow Capacity (m^3/s)	Inlet velocity (m/s)	Geometry	Average velocity in turbine section (m/s)	Water surface condition	Velocity increment (m/s)
0.1	0.18	Damper plate with nozzle	2.35	No spillage	13.06
		Without damper plate with nozzle	2.32	No spillage	12.89
		Damper plate without nozzle	2.59	Starving debit	14.39
		Without damper plate and nozzle	**2.91**	**No spillage**	**16.17**
0.2	0.36	Damper plate with nozzle	2.47	Spillage	6.86
		Without damper plate with nozzle	2.41	Spillage	6.69
		Damper plate without nozzle	**3.51**	**No spillage**	**9.75**
		Without damper plate and nozzle	2.91	Spillage	8.08

Furthermore, as the radius decreased, the color became brighter in the tangential velocity contour distribution. It was also evident that the concentration of bright color contours was in the transformer section. Figure 12 shows the graph of tangential velocity distribution at three observation heights. The graph indicated that the highest velocity was obtained at the height of 0.4 meters, where the velocity magnitude value was 5.525 m/s at *Z* position of -0.131 m. As the radius decreased, the velocity decreased since the middle area was filled with air.

The velocity graph along the wall area at *Z* position of -0.131 m in Figure 13 also supported this highest velocity result. Figure 13 shows that at around a height of 0.433 meters, the formed near wall velocity is 5.799 m/s. Upon further observation of the graph, the high-velocity area is between a height of 0.267 to 0.7 meters, with values above 2 m/s. Considering the water phase concentration at that height range, according to Figure 7, which was the transformer area, it was highly possible to install an impulse turbine in that area due to the high tangential velocity and high-water phase concentration, providing enough mass and velocity to generate sufficient momentum to rotate the turbine. Additionally, placing the turbine in the transformer section was crucial to allow the flow to develop its tangential kinetic energy in the vortex generator, resulting in increased energy conversion.

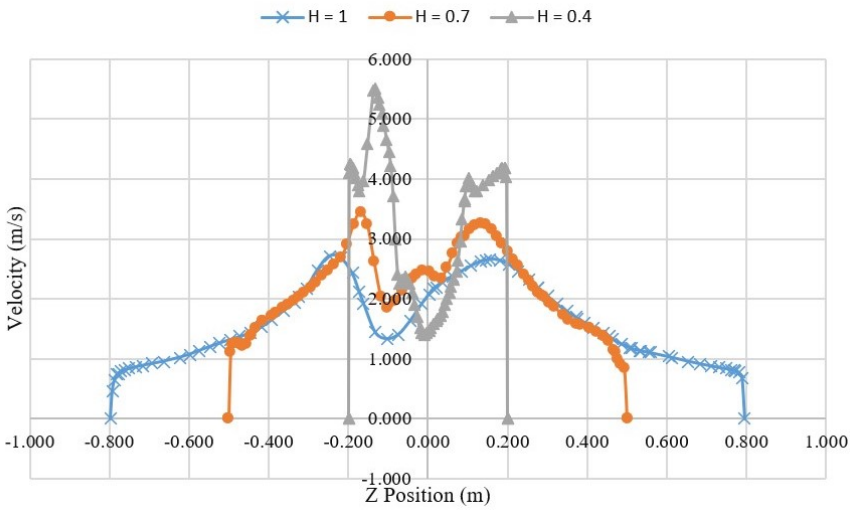

Figure 12. Velocity on three different heights across geometry radius on basin design with damper plate without nozzle at flow capacity of 0.2 m^3/s.

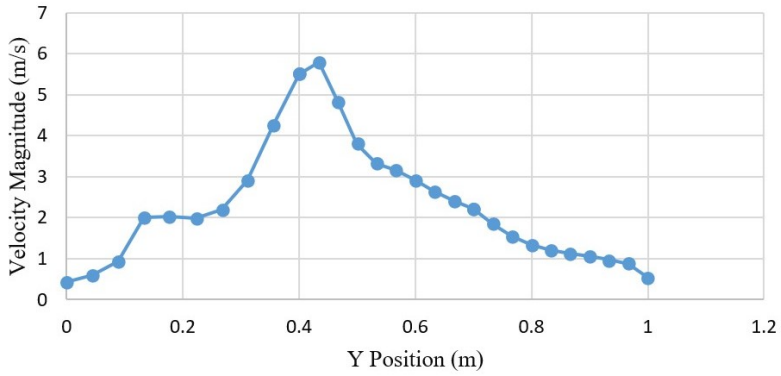

Figure 13. Near wall velocity graph of basin with damper plate without nozzle at flow capacity of 0.2 m^3/s.

4. Conclusion

The first conclusion drawn from various numerical simulations of different basin designs is that the nozzle's presence does not produce the intended suction effect and obstructs the flow, evident from the low average velocity values with nozzles. The second conclusion is that a damper plate is an additional feature that may enhance or impede the basin design's flow results. In a basin design with a capacity of 0.1 m^3/s, installing a damper plate decreased the final velocity formed to 2.59 m/s. On the other hand, removing the damper plate increased the velocity to 2.91 m/s. For a 0.2 m^3/s capacity, the absence of a damper plate caused the flow to spill, and the final velocity was only 2.91 m/s, whereas installing a damper plate maximized the flow, and the final velocity increased to 3.51 m/s. Finally, an impulse turbine can be added to the transformer section to take advantage of the rotating flow and convert it into a vortex.

References

[1] BPS, "Rata-rata harian aliran sungai, tinggi aliran, dan volume air di beberapa sungai yang daerah pengalirannya lebih dari 100 km persegi." pp. 6–8, 2015. https://www.bps.go.id/statictable/2017/11/14/1984/.

[2] K. Brown, "Power generating method and apparatus," 1968.

[3] A. B. Timilsina, S. Mulligan, and T. R. Bajracharya, "Water vortex hydropower technology: a state-of-the-art review of developmental trends," *Clean Technologies and Environmental Policy*, vol. 20, no. 8, pp. 1737–1760, 2018.

[4] S. Wanchat, R. Suntivarakorn, S. Wanchat, K. Tonmit, and P. Kayanyiem, "A parametric study of a gravitation vortex power plant," in *Advanced Materials Research*, vol. 805–806, pp. 811–817, Trans Tech Publ, May 2013.

[5] C. Power, A. McNabola, and P. Coughlan, "A parametric experimental investigation of the operating conditions of gravitational vortex hydropower (GVHP)," *Journal of Clean Energy Technologies*, vol. 4, no. 2, pp. 112–119, 2016.

[6] S. Dhakal, A. B. Timilsina, R. Dhakal, D. Fuyal, T. R. Bajracharya, H. P. Pandit, N. Amatya, and A. M. Nakarmi, "Comparison of cylindrical and conical basins with optimum position of runner: Gravitational water vortex power plant," *Renewable and Sustainable Energy Reviews*, vol. 48, pp. 662–669, Aug. 2015.

[7] R. Dhakal, S. Shrestha, H. Neupane, S. Adhikari, and T. Bajracharya, "Inlet and outlet geometrical condition for optimal installation of gravitational water vortex power plant with conical basin structure," in *Recent Advances in Mechanical Infrastructure: Proceedings of ICRAM 2019*, pp. 163–174, Springer, Nov. 2020.

[8] E. M. Wardhana, A. Santoso, and A. R. Ramdani, "Analysis of gottingen 428 airfoil turbine propeller design with computational fluid dynamics method on gravitational water vortex power plant," *International Journal of Marine Engineering Innovation and Research*, vol. 3, no. 3, 2019.

[9] D. Powalla, S. Hoerner, O. Cleynen, N. Müller, J. Stamm, and D. Thévenin, "A computational fluid dynamics model for a water vortex power plant as platform for etho-and ecohydraulic research," *Energies*, vol. 14, no. 3, p. 639, 2021.

[10] H. K. Versteeg, W. Malalasekera, G. Orsi, J. H. Ferziger, A. W. Date, and J. D. Anderson, "An introduction to computational fluid dynamics: the finite volume method." Harlow Essex: Longman Group Ltd., 1995.

[11] ANSYS Fluent, *ANSYS Fluent Theory Guide*, Nov. 2013. ANSYS Inc., USA, pp. 724–746.